



Universiteit
Leiden
The Netherlands

Upconverting nanovesicles for the activation of ruthenium anti-cancer prodrugs with red light

Askes, S.H.C.

Citation

Askes, S. H. C. (2016, November 24). *Upconverting nanovesicles for the activation of ruthenium anti-cancer prodrugs with red light*. Retrieved from <https://hdl.handle.net/1887/44378>

Version: Not Applicable (or Unknown)

License: [Licence agreement concerning inclusion of doctoral thesis in the Institutional Repository of the University of Leiden](#)

Downloaded from: <https://hdl.handle.net/1887/44378>

Note: To cite this publication please use the final published version (if applicable).

Cover Page



Universiteit Leiden



The handle <http://hdl.handle.net/1887/44378> holds various files of this Leiden University dissertation.

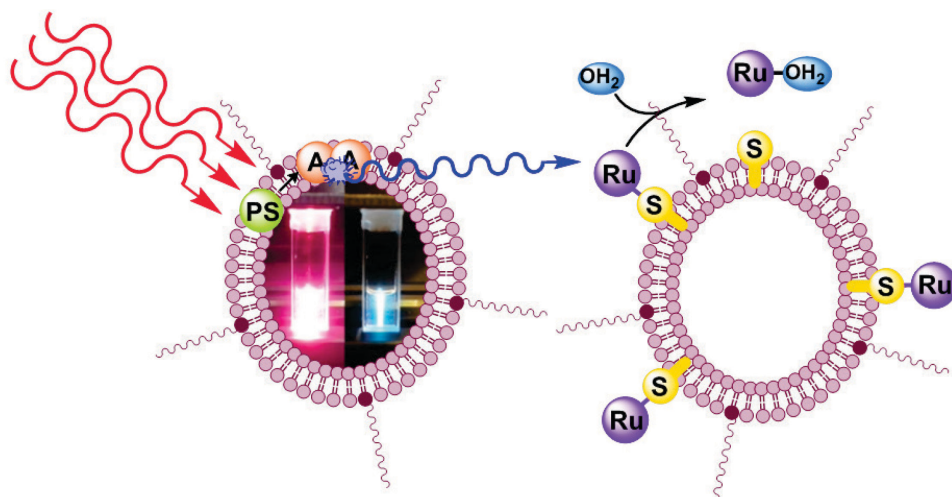
Author: Askes, S.H.C.

Title: Converting nanovesicles for the activation of ruthenium anti-cancer prodrugs with red light

Issue Date: 2016-11-24

CHAPTER 3

Activation of a photodissociative ruthenium complex by triplet-triplet annihilation upconversion in liposomes



Liposomes capable of generating blue photons in situ by triplet-triplet annihilation upconversion of either green or red light, were prepared. The red-to-blue upconverting liposomes were capable of triggering the photodissociation of ruthenium polypyridyl complexes from PEGylated liposomes using a clinical grade PDT laser source (630 nm).

This chapter was published as a communication: S. H. C. Askes, A. Bahreman, S. Bonnet, *Angew. Chem., Int. Ed.* **2014**, 53, 1029-1033.

3.1 Introduction

Light-sensitive ruthenium(II) polypyridyl compounds are classical tools in photochemistry that have recently been proposed as prodrugs for photoactivatable anticancer therapy (PACT).^[1] As shown in classical photodynamic therapy (PDT), the use of light to treat cancer allows for spatially and temporally controlling the toxicity of an anticancer drug, which lowers side effects for cancer patients. Meanwhile, loading anticancer drugs into drug carriers such as liposomes helps targeting the compounds to tumor tissues. Especially sterically hindered liposomes, *i.e.*, those grafted with polyethylene glycol chains, have been recognized as versatile and biocompatible drug carriers for the treatment of various diseases because of their long lifetime in the blood circulation. With such PEGylated liposomes uptake in tumors is enhanced due to the so-called enhanced permeability and retention (EPR) effect.^[2] In PACT, activation of for example ruthenium-functionalized liposomes could be realized after cell uptake using visible light. However, most ruthenium(II) polypyridyl compounds require activation with blue light (400 – 500 nm), *i.e.*, outside the phototherapeutic window (600 – 1000 nm), in which light permeates mammalian tissues optimally. In this work, *in situ* upconversion of red to blue light is realized using triplet-triplet annihilation upconversion (TTA-UC), and combined with ruthenium-functionalized liposomes to trigger the activation of the ruthenium complex using a clinical grade PDT laser source.

In TTA-UC, low energy photons are converted into higher energy photons by means of a bimolecular mechanism involving a sensitizer and two annihilator molecules.^[3] The sensitizer absorbs the low-energy light, undergoes intersystem crossing (ISC) to a triplet state, and transfers its energy to an annihilator molecule *via* triplet-triplet energy transfer (TTET). Collision of two triplet annihilator molecules leads to triplet-triplet annihilation (TTA), whereby one molecule is promoted to the excited singlet state, while the other one falls back to the ground state. The singlet annihilator returns to the ground state by emission of a high-energy photon, thus realizing upconversion. TTA-UC with a range of molecule pairs has been realized in organic solvent,^[3a, 3b, 3d] ionic liquid,^[4] polymers,^[3a, 3c, 5] and various water-soluble nanoparticles.^[6] In this communication, we demonstrate the first examples of TTA-UC in the lipid bilayer of neutral liposomes.

3.2 Results and discussion

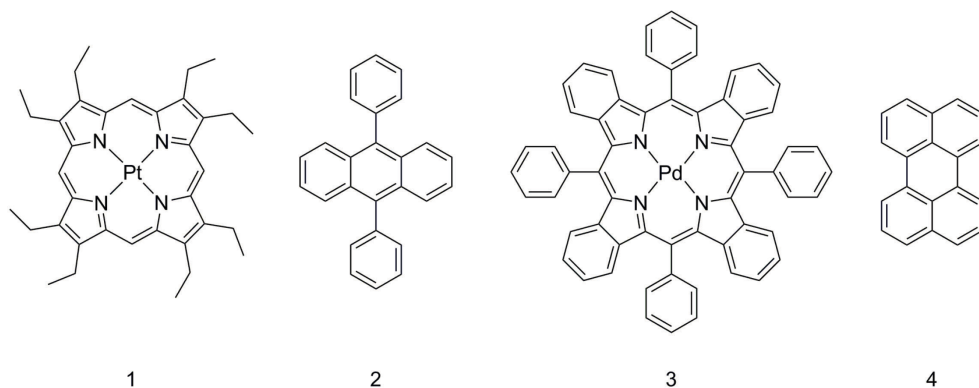


Figure 3.1. Chemical structures of platinum octaethylporphyrin (**1**), 9,10-diphenylanthracene (**2**), palladium tetraphenyltetrabenzoporphyrin (**3**), and perylene (**4**).

Two well-investigated TTA-UC couples were considered for incorporation in liposomes: platinum octaethylporphyrin (**1**) and 9,10-diphenylanthracene (**2**) on the one hand, and palladium tetraphenyltetrabenzoporphyrin (**3**) and perylene (**4**) on the other hand (Figure 3.1). Obviously, when included in liposomes these highly apolar molecules favor the lipophilic interior of the lipid bilayer. Liposomes made of 1,2-dimyristoyl-*sn*-glycero-3-phosphocholine (DMPC) and containing 4 mol% of sodium N-(carbonyl-methoxypolyethylene glycol-2000)-1,2-distearoyl-*sn*-glycero-3-phosphoethanolamine (DSPE-MPEG-2000), the sensitizer **1** or **3**, and/or the annihilator **2** or **4**, were prepared by extrusion in DPBS buffer solution (Table 3.1). The diameters of the liposomes (130 – 170 nm) were measured by dynamic light scattering. UV-VIS absorption and luminescence spectra of liposomes containing either the sensitizer or the annihilator, *i.e.*, of samples **L1**, **L2**, **L3**, and **L4**, were comparable to that of the corresponding compounds in toluene solution (Figure S.II.1). Thus, incorporation of any of the four molecules shown in Figure 3.1 into the DMPC bilayers did not change their spectroscopic properties.

Although in liposome samples **L1-2** and **L3-4** both molecules of each upconverting couple were successfully inserted into the bilayer, it was initially uncertain whether their diffusion in the two-dimensions of the bilayer would be sufficient to allow TTA-UC to occur.^[3a] After deoxygenation these samples were excited at either 532 nm or 630 nm, respectively, near the absorption maximum of the highest Q-band of **1** ($\lambda_{\text{max}} = 536$ nm) or **3** ($\lambda_{\text{max}} = 628$ nm),

Chapter 3

respectively. A bright blue luminescence was observed in both cases (Figure 3.2) after suppressing the scattered excitation light with notch and/or short pass filters. Under the same experimental conditions, no blue emission was observed for **L1**, **L2**, **L3**, or **L4**, thus proving that both components of each upconverting couple are necessary for the upconversion to occur. To the best of our knowledge, **L1-2** and **L3-4** are the first examples showing TTA-UC in liposomes. As both green-to-blue and red-to-blue upconversion was obtained, the use of liposomes appears to be a straightforward manner to solubilize TTA-UC couples in aqueous solution.

Table 3.1. Overview of liposomal formulations used in this work. [DMPC], [PEG], [1], [2], [3], [4] and [5] represent the bulk concentrations in DMPC, DSPE-MPEG-2000, **1**, **2**, **3**, **4** and **5**²⁺, respectively, in DPBS buffer.

Code	[DMPC] (mM)	[DSPE-mPEG-2000] (mM)	[1] (μ M)	[2] (μ M)	[3] (μ M)	[4] (μ M)	[5] (mM)
L1-2	20	0.80	3.5	100	-	-	-
L1	20	0.80	3.5	-	-	-	-
L2	20	0.80	-	100	-	-	-
L3-4	20	0.80	-	-	2.5	50	-
L3	20	0.80	-	-	2.5	-	-
L4	20	0.80	-	-	-	50	-
L5	5.0	0.20	-	-	-	-	0.20

The luminescence spectra of **L1-2** and **L3-4** were measured at 298 K under argon (Figure 3.3). Upon excitation at 532 nm, **L1-2** shows a structured upconversion band at 433 nm, corresponding to emission of **2** in toluene (Figure S.II.1b). A second band was present as well; its emission maximum (646 nm) was consistent with the phosphorescence of **1** in toluene (Figure S.II.1a). Similarly, for **L3-4** excitation at 630 nm leads to an upconversion band at 473 nm, and a second band at 800 nm (Figure 3.3). The upconversion emission corresponds to emission of **4** in toluene (Figure S.II.1d), apart from the first peak at 447 nm that was filtered by the 633 nm notch filter used for rejecting the scattered excitation (Figure S.II.2). The peak at 800 nm in the emission spectrum of **L3-4** corresponds to the phosphorescence of **3**, as observed in toluene (Figure S.II.1c). In both samples, the phosphorescence band corresponds to a unimolecular event, *i.e.*, emission from a photosensitizer molecule in the triplet state, whereas the upconversion band derives from bimolecular events leading to emission from an annihilator in the singlet state.

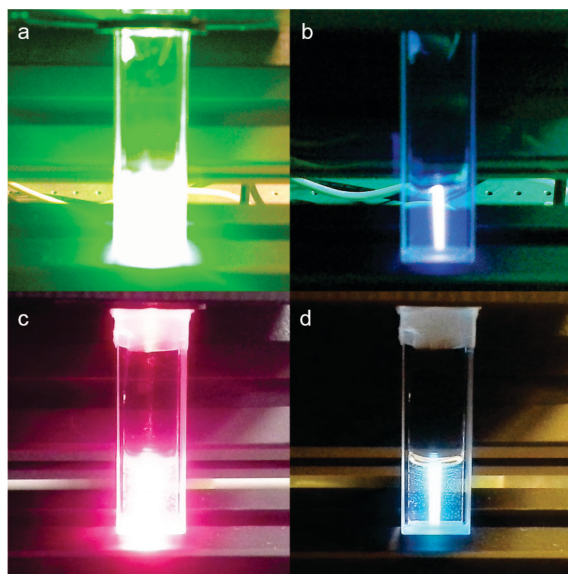


Figure 3.2. Digital photographs of **L1-2** and **L3-4** under irradiation at 532 nm and 630 nm, respectively, with 27 mW excitation power (for both systems) in a 2.6 mm diameter beam (intensity: 0.51 W.cm^{-2}). (a) **L1-2** without filter. (b) **L1-2** with 533 nm notch filter and $<575 \text{ nm}$ short pass filter. (c) **L3-4** without filter. (d) **L3-4** with 633 nm notch filter. Samples were deoxygenated and maintained at 298 K.

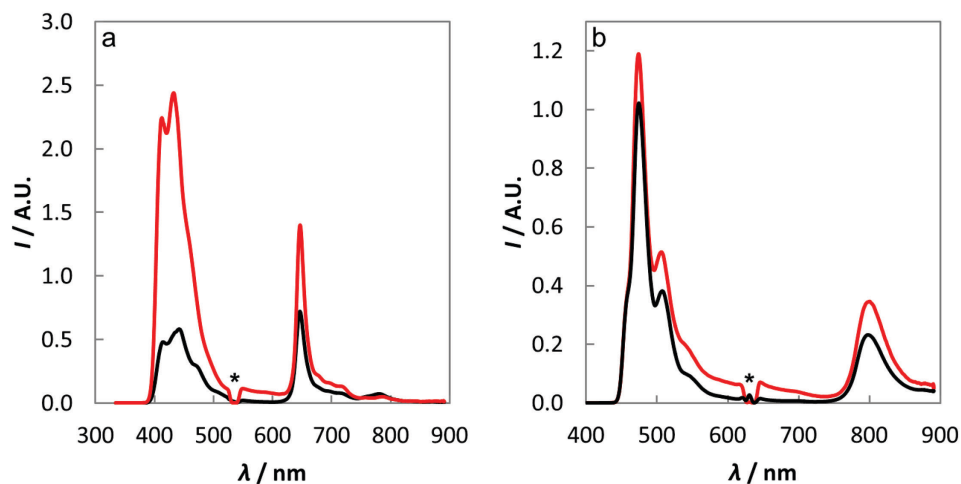


Figure 3.3. (a) Emission spectra of liposome sample **L1-2** (black) and of a toluene solution containing **1** and **2** at the same bulk concentrations (red, $[\mathbf{1}] = 3.5 \mu\text{M}$ and $[\mathbf{2}] = 100 \mu\text{M}$). (b) Emission spectra of the liposome sample **L3-4** (black) and of a toluene solution containing **3** and **4** at the same bulk concentrations (red, $[\mathbf{3}] = 2.5 \mu\text{M}$ and $[\mathbf{4}] = 50 \mu\text{M}$). Asterisks indicate excitation (532 nm for **L1-2** and 630 nm for **L3-4**). The samples were deoxygenated before measurement. Spectra acquired at 298 K, excitation power for both samples 27 mW, 2.6 mm diameter beam, intensity 0.51 W.cm^{-2} .

Chapter 3

The luminescence spectra of both upconverting couples were measured in toluene using the same bulk concentrations for the sensitizer and annihilator as for **L1-2** and **L3-4**. The upconversion intensity for couple **1-2** was found to be four times weaker in liposomes than in toluene at 298 K, and for couple **3-4** it was comparable for both sample types (Figure 3.3). Upon inserting the sensitizer and annihilator in the lipid bilayer two phenomena take place simultaneously. On the one hand, compartmentalization of the lipophilic molecules in the bilayer increases their local concentrations, which increases the probability of intermolecular collisions and therefore the rates of TTET and TTA. On the other hand, two-dimensional diffusion in a lipid bilayer is somewhat slower than in a non-viscous isotropic toluene solution, which may decrease TTA-UC efficiency in liposomes. Overall, our data show that the trade-off is excellent and that efficient TTA-UC occurs in PEGylated DMPC liposomes (at 298 K).

Table 3.2. Upconversion quantum yield (Φ_{uc}) in liposomes and toluene at 293 K.

TTA-UC Couple	Φ_{uc} (%)	
	in PEGylated DMPC liposomes	in toluene
1-2 ^[a]	2.3 (L1-2)	5.1 ^[b]
3-4 ^[c]	0.5 (L3-4)	1.2 ^[d]

[a] 532 nm, 10 mW excitation power, 1.5 mm diameter beam (intensity 0.57 W.cm⁻²). [b] [**1**] = 3.5 μ M, [**2**] = 100 μ M. [c] 630 nm, 10 mW excitation power, 2.5 mm diameter beam (intensity 0.20 W.cm⁻²). [d] [**3**] = 2.5 μ M, [**4**] = 50 μ M.

Measurements of upconversion quantum yields (Φ_{uc}) are usually done by relative actinometry.^[3a] However, intense scattering in liposome samples would make any comparison with a reference compound in homogeneous solution challenging. For this reason, the upconversion quantum yields of **L1-2** and **L3-4** were measured using an absolute method, *i.e.* with an integrating sphere and a calibrated spectrometer (Appendix I). The setup was similar to that used by Boyer *et al.* for determining the upconversion quantum yield of lanthanoid-based nanoparticles.^[7] For **L1-2**, **L3-4**, and for their toluene analogues, Φ_{uc} was determined upon irradiation using a 10 mW continuous beam (Table 3.2). At 293 K Φ_{uc} in PEGylated DMPC liposomes was found roughly half of that in toluene for both couples, with values of 2.3% and 0.5% for **L1-2** and **L3-4**, respectively, *versus* 5.1% and 1.2% in toluene. To the best of our knowledge, this is the first time that the quantum yield of TTA-UC has been determined using an absolute method.

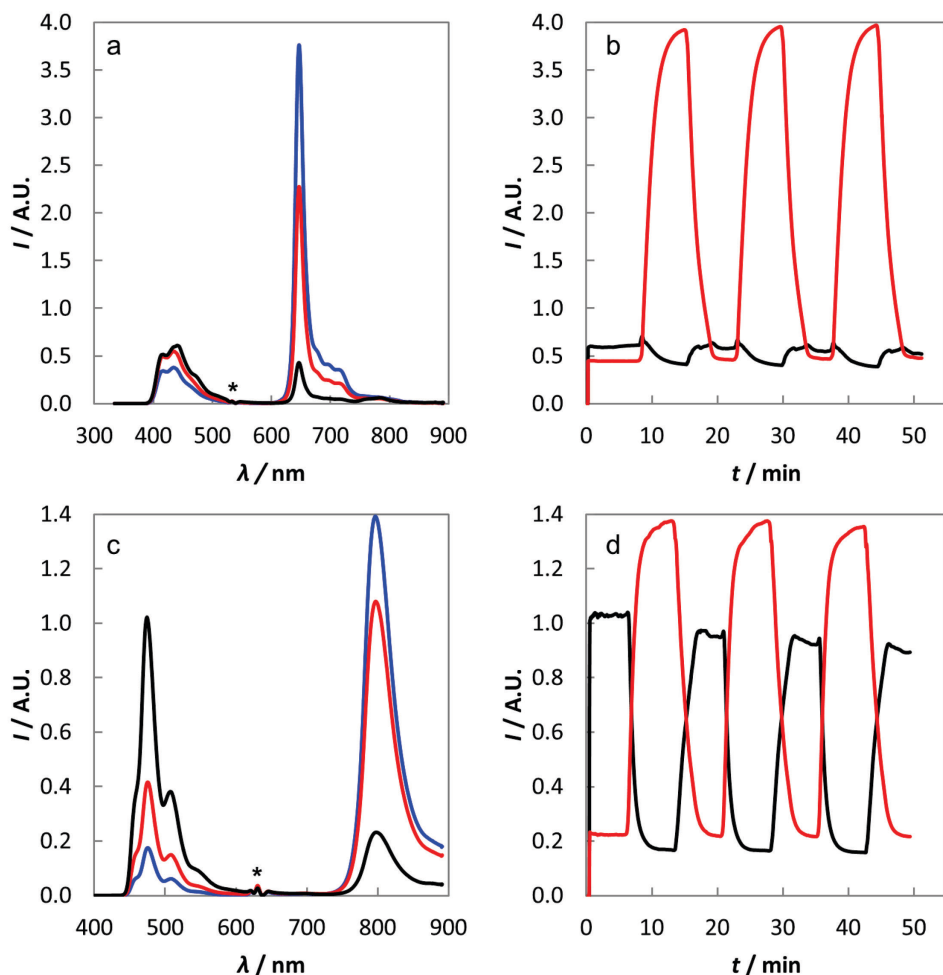


Figure 3.4. (a) Luminescence spectrum of **L1-2** at 288 K (blue), 293 K (red) and at 298 K (black). (b) Time dependency of the upconversion at 436 nm (black) and of the phosphorescence at 646 nm (red) of **L1-2** during three warming and cooling cycles from 288 to 298 K and from 298 to 288 K. (c) Luminescence spectrum of **L3-4** at 288 K (blue), 293 K (red) and 298 K (black). (d) Time dependency of the upconversion at 473 nm (black) and of the phosphorescence at 800 nm (red) of **L3-4** during three warming and cooling cycles from 288 to 298 K and from 298 to 288 K. Asterisks indicate excitation wavelengths (532 nm for **L1-2** and 630 nm for **L3-4**). Samples were deoxygenated before measurement. Excitation power for both samples: 27 mW, 2.6 mm diameter beam, intensity 0.51 W.cm^{-2} .

The TTA-UC process is diffusion controlled, and therefore depends on temperature. For this reason, luminescence spectra were measured for **L1-2** and **L3-4** at 288, 293, and 298 K (Figure 3.4a and Figure 3.4c). Upon warming, the sensitizer phosphorescence decreased for both samples, while the upconversion emission increased markedly. In contrast, for toluene samples at

Chapter 3

the same bulk concentrations both the upconversion and phosphorescence intensities slightly decreased with increasing temperatures (Figure S.II.3) as a result of faster non-radiative decay. The liposome samples were subjected to three warming-cooling cycles while continuously monitoring their luminescence (Figure 3.4b and Figure 3.4d). The temperature dependence of the upconversion was found to be reversible, which advocates for a reversible, physical cause rather than an irreversible chemical evolution (such as aggregation or photoreactions of the chromophores). As the change of the upconversion vs. phosphorescence ratio occurs at a temperature that fits the gel-to-fluid phase transition temperature (T_m) of DMPC membranes (296.9 K), we interpret this change as a consequence of the much increased translational diffusion coefficient (D_T) of membrane-embedded molecules above T_m , compared to that at temperatures below T_m .^[8] TTET and TTA are both expected to occur much more frequent in the liquid phase of the membrane, *i.e.*, above T_m , which would lead to an increase in the probability of upconversion (an intermolecular process) at the cost of phosphorescence (a monomolecular process). Similar observations were made for TTA-UC in rubbery polymer matrixes by Sing-Rachford and co-workers.^[5e]

In order to prove that *in situ* upconverted blue photons may be used to activate light-activatable prodrugs using red light, ruthenium-functionalized liposomes were mixed with the upconverting liposomes **L3-4** (Figure 3.5b). The ruthenium complex $[\text{Ru}(\text{tpy})(\text{bpy})(\text{SRR}')]\text{2}^+$ (**5**²⁺, see Figure 3.5a and experimental section) was selected because it has a single light-sensitive Ru-S bond. This kind of photoactivatable ruthenium compound shows stability in the dark but hydrolyzes to the aqua species $[\text{Ru}(\text{tpy})(\text{bpy})(\text{H}_2\text{O})]\text{2}^+$ (**6**²⁺) upon irradiation with blue light into its Metal-to-Ligand Charge Transfer state.^[9] A thioether-cholesterol ligand (SRR') can be used to anchor the complex to lipid bilayers, as has been demonstrated in our group.^[9a, 9c] PEGylated DMPC liposomes bearing 3.7 mol% of complex **5**²⁺ were prepared (sample **L5**, Table 3.1) and added in 1:1 volumetric ratio to the red-to-blue upconverting liposome sample **L3-4**. Both types of liposomes being grafted with sterically hindering polyethylene glycol (PEG) tails, fusion of the liposomes does not occur, and only radiative energy transfer between the upconverting liposomes and the ruthenium-functionalized liposomes should take place (Figure 3.5b).^[10]

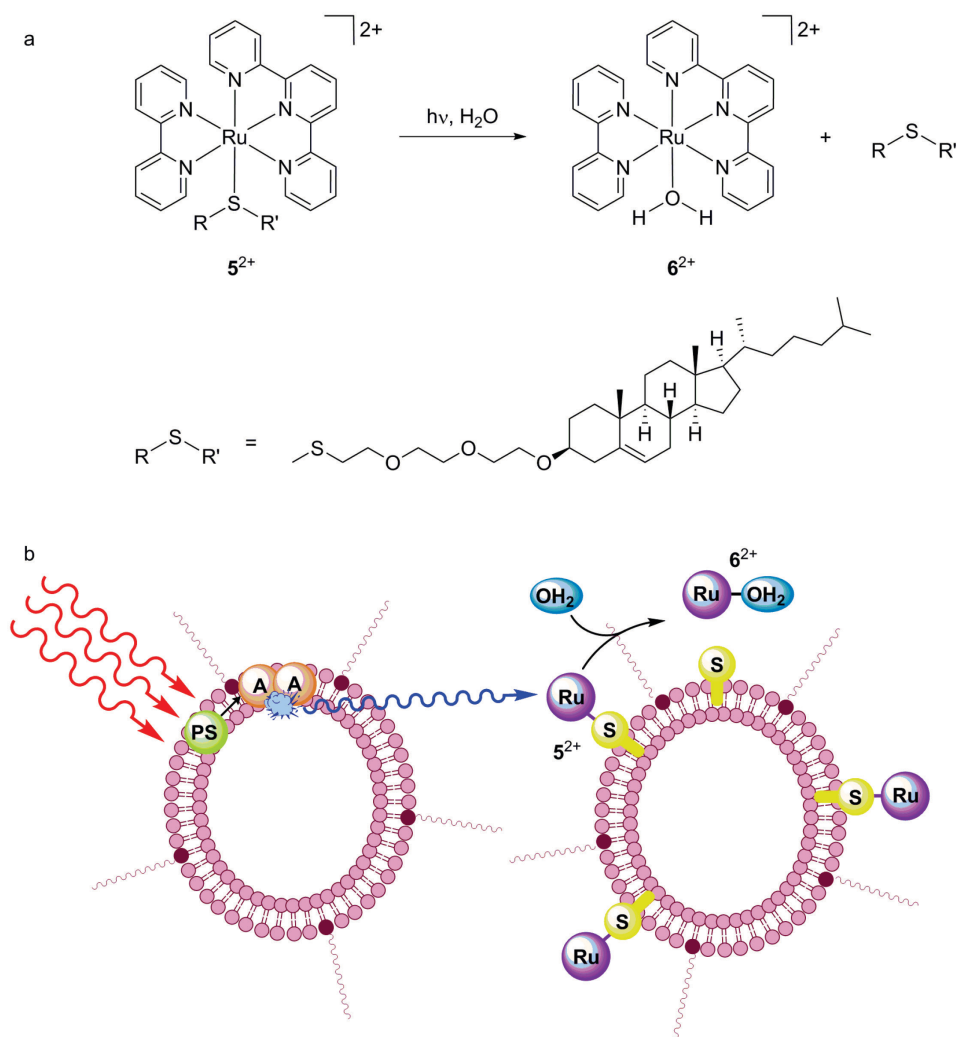


Figure 3.5. (a) Chemical structures of 5^{2+} and 6^{2+} and the conversion of 5^{2+} into 6^{2+} . (b) Cartoon illustrating the TTA-UC process in the lipid bilayer, using a photosensitizer (PS) and an annihilator (A). Radiative energy transfer from the annihilator to complex 5^{2+} , indicated with a blue arrow, triggers light-induced hydrolysis of 5^{2+} to release 6^{2+} in solution.

The liposome mixture was deoxygenated and irradiated at 298 K for 2 hours with a 120 mW 630 nm laser light beam from a clinical grade Diomed PDT laser. The photoreaction was monitored by UV-vis spectroscopy at fixed intervals during irradiation (Figure 3.6). Although the absorbance of **4** dominates the spectrum, the characteristic band of the hydrolyzed photoproduct (6^{2+}) could clearly be seen, rising between 450 and 550 nm as a

function of irradiation time. The isosbestic point at 457 nm showed that a single photochemical process was taking place. Monitoring the absorbance at 490 nm allowed for quantitatively measuring the build-up of 6^{2+} as a function of irradiation time, which reached a plateau after 3 hours irradiation (Figure 3.6b). As a control experiment, a mixture of liposomes **L4** and **L5** was irradiated under the same experimental conditions as above. In liposomes **L4** the absence of sensitizer prevents upconversion from occurring, and the red photons can only excite the ruthenium complex by direct absorption in the tail of the $^1\text{MLCT}$ band. The extinction coefficient of 5^{2+} being very low at 630 nm ($\epsilon \leq 100 \text{ M}^{-1}\cdot\text{cm}^{-1}$), even under a strong photon flux the photoconversion to 6^{2+} was much slower than in presence of **L3-4** (Figure 3.6b), *i.e.*, the upconverting liposomes achieve efficient sensitization of the photosubstitution reaction. A second control experiment showed that no photodissociation occurred in absence of light. Overall, these data are the first evidence that blue photons produced *in situ* by upconversion of PDT-compatible red photons, can be used to enhance the photodissociation rate of polypyridyl ruthenium complexes.

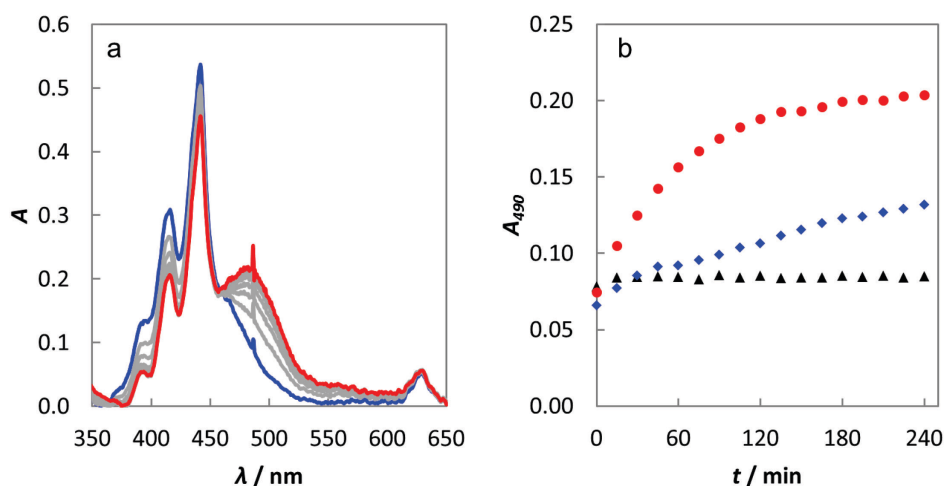


Figure 3.6. (a) Absorption spectra, after baseline correction, of a 1:1 vol% mixture of liposome samples **L3-4** and **L5** (Table 3.1) during red light irradiation (630 nm). Blue line: spectrum at $t = 0$; red line: spectrum at $t = 240$ min; grey lines: spectra measured every 30 min. (b) Plot of the absorbance at 490 nm during red light irradiation (630 nm) of a 1:1 vol% mixture of **L3-4** and **L5** (red dots), of a 1:1 vol% mixture of **L4** and **L5** (blue diamonds), and absorbance at 490 nm of a 1:1 vol% mixture of **L4** and **L5** left in the dark (black triangles). Irradiation conditions: power 120 mW, beam diameter 2.6 mm, intensity $2.3 \text{ W}\cdot\text{cm}^{-2}$, $T = 298 \text{ K}$, sample volume 1 mL.

3.3 Conclusion

In conclusion, triplet-triplet annihilation upconversion was for the first time realized in PEGylated liposomes and characterized by absolute quantum yield

measurement. Red-to-blue upconverting liposomes **L3-4**, when mixed with ruthenium-functionalized, PEGylated liposomes **L5** and irradiated with a clinical grade PDT laser at 630 nm, were able to trigger *via* radiative energy transfer the hydrolysis of the Ru-S bond and to release complex **6²⁺**. The upconverting liposomes transform two low-energy photons, which penetrate far in biological tissues but are poorly absorbed by the ruthenium complex, into one blue photon that does not need to travel into tissues and can directly promote the complex into its photoreactive excited state. Metal-ligand photodissociation mediated by upconverted light represents exciting perspectives for photoactivatable chemotherapy in oxygen-poor tissues such as hypoxic tumors. Obviously, the oxygen sensitivity of TTA-UC in liposomes needs to be addressed before concluding on the practical application of such systems *in vivo*. However, the high quantum yield of TTA-UC in liposomes and the excellent molar absorptivity of porphyrin sensitizers, for example compared to lanthanoid-based upconverting nanoparticles, may offer fascinating applications in bio-imaging, photoactivatable chemotherapy, and other applications where the *in situ* generation of blue light is required.

3.4 Experimental section

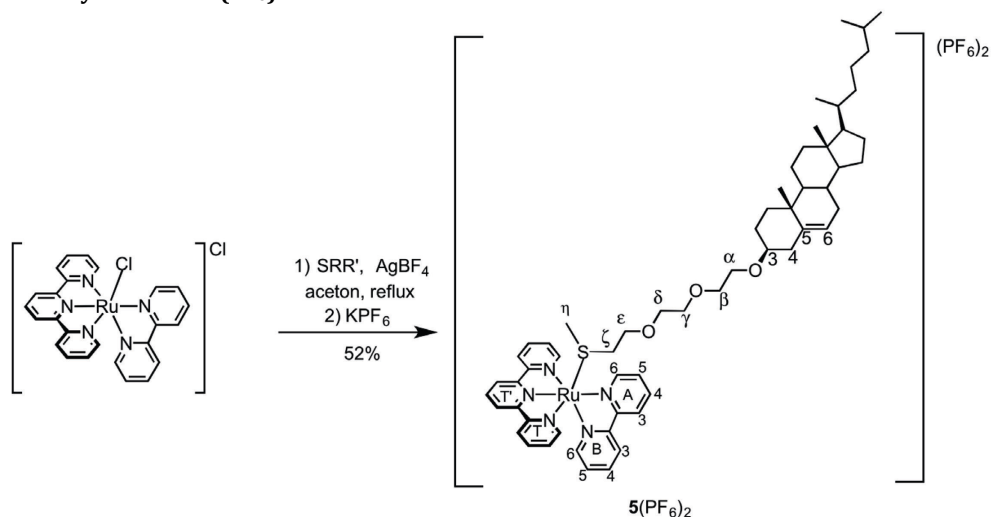
3.4.1 General

Platinum octaethylporphyrin (**1**) and palladium tetraphenyl tetrabenzoporphyrin (**3**) were purchased from Frontier Scientific, Inc. (Logan, Utah, USA). Diphenyl anthracene (**2**) was purchased from Alfa Aesar GmbH & Co KG (Karlsruhe, Germany). Perylene (**4**) was purchased from Sigma-Aldrich Chemie BV (Zwijndrecht, The Netherlands). Sodium N-(carbonyl-methoxypolyethylene glycol-2000)-1,2-distearoyl-*sn*-glycero-3-phosphoethanolamine (DSPE-MPEG-2000) and 1,2-dimyristoyl-*sn*-glycero-3-phosphocholine (DMPC) were purchased from Lipoid GmbH (Ludwigshafen, Germany) and stored at -18 °C. Dulbecco's phosphate buffered saline (DPBS) was purchased from Sigma Aldrich and had a formulation of 8 g.L⁻¹ NaCl, 0.2 g.L⁻¹ KCl, 0.2 g.L⁻¹ KH₂PO₄, and 1.15 g.L⁻¹ K₂HPO₄ with a *pH* of 7.1-7.5. All chemicals were used as received. The syntheses of the thioether-cholesterol conjugate SRR' and [Ru(terpy)(bpy)(Cl)](Cl) are described elsewhere.^[9c, 11]

Regular UV-Vis absorption spectra were taken on a Varian Cary 50 UV-Vis spectrometer. Emission spectra with excitation wavelengths 416 and 378 nm were taken on a Shimadzu RF-5301PC spectrofluorimeter at ambient atmosphere. Emission spectra with excitation wavelengths 532 nm and 630 nm were measured in the same setup as for upconversion emission spectrometry, detailed below, and were always collected from deoxygenated samples that had been thoroughly bubbled with argon (Argon 4.6, LindeGas) for at least 30 minutes with a rate of ~2 bubbles per second.

Chapter 3

3.4.2 Synthesis of **5**(PF₆)₂



Scheme 3.1. Synthesis of **5**(PF₆)₂

[Ru(tpy)(bpy)(Cl)](Cl) (100 mg, 0.18 mmol), ligand SRR' (117 mg, 0.21 mmol), and AgBF₄ (73 mg, 0.37 mmol) were dissolved in acetone (30 mL). The reaction mixture was refluxed for 20 h in the dark. After cooling to room temperature it was filtered hot over Celite, and the solvent was removed by rotary evaporator under reduced pressure. The product was purified by column chromatography on silica gel (acetone/H₂O/sat. aq. KPF₆ 100:10:1.5, R_f = 0.35). Acetone was evaporated under vacuum, upon which the product precipitated as an orange solid. **5**(PF₆)₂ was filtered, washed with water and dried under vacuum for 4 h. (124 mg, 52%). ¹H NMR (300 MHz, δ in CDCl₃) 9.72 (d, J = 5.3 Hz, 1H, A6), 8.55 (m, J = 8.2 Hz, 3H, A3 + T3'), 8.41 (d, J = 7.9 Hz, 2H, T3), 8.34 (d, J = 8.0 Hz, 1H, B3), 8.27 – 8.14 (m, 2H, A4 + T4'), 8.03 – 7.85 (m, 3H, A5 + T4), 7.74 (t, 1H, B4), 7.68 (d, J = 5.0 Hz, 2H, T6), 7.36 (m, 2H, B5 + B6), 7.16 (m, 2H, T5), 5.30 (d, J = 4.8 Hz, 1H, 6), 3.75 (t, J = 6.6 Hz, 2H, ζ), 3.64 – 3.37 (m, 10H, α + β + γ + δ + ε), 3.13 (s, 1H, 3), 2.40 – 0.75 (m, 47H), 0.67 (s, 3H). ¹³C NMR (75 MHz, δ in CDCl₃) 157.67 + 157.01 + 156.31 + 156.29 (B2 + A2 + T2 + T2'), 153.18 (T6), 151.95 (A6), 149.80 (B6), 140.86 (5), 139.09 (T4), 138.56 + 138.37 (B4 + A4), 137.56 (T4'), 128.91 (T5), 128.35 (A5), 127.87 (B5), 125.16 (T3), 124.85 (A3), 124.48 (T3'), 124.03 (B3), 121.86 (6), 79.56 (3), 70.88 + 70.35 + 70.30 + 67.52 + 67.30 (α + β + γ + δ + ε), 56.86, 56.28, 50.26, 42.44, 39.88, 39.64, 39.22, 37.28, 36.97, 36.31, 35.91, 34.47, 32.06, 32.01, 29.82, 28.35, 28.13, 24.42, 23.97, 22.95, 22.69, 21.19, 19.53, 18.85, 15.04, 12.00. UV-Vis: λ_{max} (ε in L.mol⁻¹.cm⁻¹) in CHCl₃: 457 nm (6090). ES MS m/z exp. (calc.): 519.7 (519.4, [M-2PF₆]²⁺). Elemental analysis for C₅₉H₇₉F₁₂N₅O₃P₂RuS: (calc.); C, 53.31; H, 5.99; N, 5.27; S, 2.41. (Found); C, 53.34; H, 6.22; N, 5.15; S 2.41.

3.4.3 Liposome preparation

All liposome formulations were prepared by the classical hydration-extrusion method. As an example, the preparation of **L1-2** is described here. Aliquots of chloroform stock solutions containing the liposome constituents were added together in a flask to obtain a solution with 20 μmol DMPC, 0.8 μmol DSPE-MPEG-2000, 100 nmol **2**, and 3.5 nmol **1**. The organic solvent was removed by rotary evaporation and subsequently under high vacuum for at least 30 minutes to

create a lipid film. 1.0 mL DPBS buffer was added and the lipid film was hydrated by 5 cycles of freezing the flask in liquid nitrogen and thawing in warm water (50 °C). The resulting dispersion was extruded through a Whatman Nuclepore 0.2 µm polycarbonate filter at 40-50 °C at least 11 times using a mini-extruder from Avanti Polar Lipids, Inc. (Alabaster, Alabama, USA). The number of extrusions was always odd to prevent any unextruded material ending up in the final liposome sample. The extrusion filter remained colorless after extrusion, suggesting complete inclusion of the TTA-UC compounds in the lipid bilayer. Liposomes were stored in the dark at 4 °C and used within 7 days. The average liposome size and polydispersity index were measured with a Malvern Instruments Zetasizer Nano-S machine, operating with a wavelength of 632 nm.

3.4.4 Setup for upconversion emission spectroscopy

Upconversion emission spectra were measured with a custom-built setup, see Figure 3.7. All optical parts were connected with FC-UVxxx-2 (xxx = 200, 400, 600) optical fibers from Avantes (Apeldoorn, The Netherlands), with a diameter of 200-600 µm, respectively, and that were suitable for the UV-Vis range (200 – 800 nm). The excitation source was either a continuous wave Aries 150 532 nm portable DPSS laser from LaserGlow (Toronto, ON, Canada), or a clinical grade Diomed 630 nm PDT laser. The 630 nm light was filtered through a FB630-10, 630 nm band pass filter (Thorlabs, Dachau/Munich, Germany) put between the laser and the sample. The excitation power was controlled using a NDL-25C-4 variable neutral density filter (Thorlabs), and measured using either a PM20 optical power meter or a S310C thermal sensor connected to a PM100USB power meter (Thorlabs). Sample deoxygenation was performed in an external ice-cooled pear-shaped flask by bubbling argon for 30 minutes with a rate of 2 bubbles per second, after which the sample was transferred to the cuvette by cannulation under argon. The sample was held under argon in a 104F-QS or 104F-OS semi-micro fluorescence cuvette from Hellma GmbH & Co. KG (Müllheim, Germany) in a CUV-UV/VIS-TC temperature-controlled cuvette holder (Avantes), and was irradiated from the top with a collimated 2.6 mm diameter beam. Emission measurement was performed by means of a 2048L StarLine CCD spectrometer from Avantes under a 90° angle with respect to excitation. The excitation light was rejected using either a NF533-17 533 nm or NF633-25 633 nm notch filter from Thorlabs.

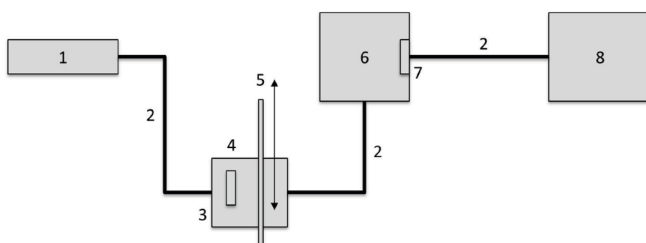


Figure 3.7. Setup used for upconversion emission spectroscopy. Legend: (1) laser source, (2) optical fibers, (3) filter holder, (4) band pass filter that can be installed or removed, (5) variable neutral density filter that can be installed or removed, (6) temperature-controlled cuvette holder, (7) notch filter, (8) CCD spectrometer.

Chapter 3

3.4.5 Photosubstitution experiments using red light

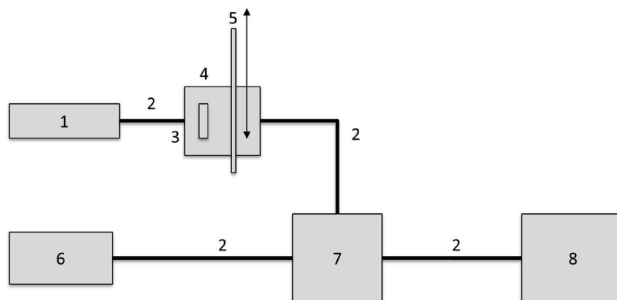


Figure 3.8. Setup used for photosubstitution experiments using red light. Legend: (1) 630 nm laser source, (2) optical fibers, (3) filter holder, (4) 630 nm band pass filter, (5) variable neutral density filter that can be installed or removed, (6) halogen-deuterium light source for absorption measurements, (7) temperature controlled cuvette holder, (8) CCD spectrometer.

Photosubstitution experiments using red light were performed with a custom build setup, see Figure 3.8. 1 mL of the liposome mixture, prepared as described in the main text, was deoxygenated by bubbling argon through the sample with a rate of ~ 2 bubbles per second for at least 30 minutes in an external ice-cooled pear-shaped flask, after which the sample was transferred by means of cannulation under argon to a 104F-QS or 104F-OS semi-micro fluorescence cuvette from Hellma GmbH & Co. KG (Müllheim, Germany) in a CUV-UV/VIS-TC temperature-controlled cuvette holder from Avantes. The sample was held under argon atmosphere at a constant temperature of 298 K and irradiated for 4 hours from the top with a 120 mW 630 nm laser light beam from a clinical grade Diomed 630 nm PDT laser. The laser was collimated to a beam of 2.6 mm diameter to reach an intensity of $2.3 \text{ W}\cdot\text{cm}^{-2}$; in such conditions, a cylinder of approximately 0.13 cm^3 was simultaneously excited by the laser. UV-Vis absorption spectra were measured using an Avalight DH-S-BAL halogen-deuterium lamp (Avantes) as light source and an 2048L StarLine spectrometer (Avantes) as detector, both connected to the cuvette holder at a 180° angle. A UV-Vis absorption spectrum was measured every 15 min; each time the laser was switched off, the halogen-deuterium lamp was turned on, a spectrum was recorded, the halogen-deuterium lamp was switched off, and the laser was switched on again. Each UV-Vis measurement took approximately 10 seconds in total. The baseline of each spectrum was corrected for Tyndall and Rayleigh scattering and drift of the halogen-deuterium light source, using Microsoft Excel 2010 and Origin 8.5 software.

3.4.6 Beam profiling

A beam profiler was used for measuring the beam diameters of the laser beams in the aforementioned setups. It consisted of a Trust Webcam Spotlight Pro, of which the front lens was pried off and replaced by NE510A (OD = 1) and NE520A (OD = 2) absorptive neutral density filters (Thorlabs). The laser beam was pointed directly on the photovoltaic chip of the webcam (4.8 mm wide and 3.6 mm high). Then, $1/e^2$ laser beam diameters in pixels were determined by Beams, an open source beam profiling software downloadable from <http://ptomato.name/opensource/beams/beams.html>. The beam diameter in millimeters was calculated by dividing the average beam diameter in pixels by the total number of horizontal pixels and multiplying this with the chip width in millimeters. For example, the diameter of the beam in Figure 3.9 was determined to be $\frac{339 \text{ px}}{640 \text{ px}} \times 4.8 \text{ mm} = 2.5 \text{ mm}$.

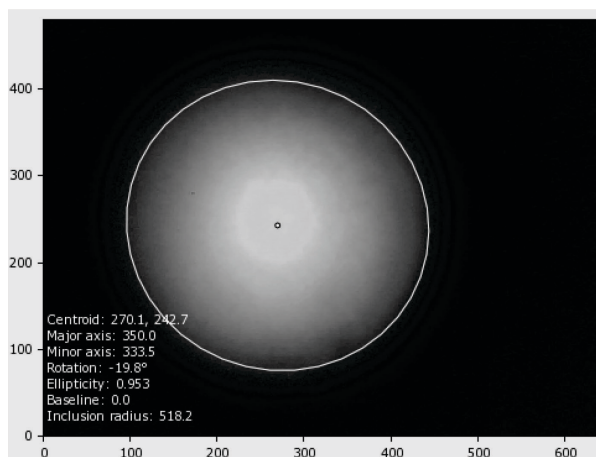


Figure 3.9. Example output generated by the beam profiling setup in combination with the Beams software package. Axes represent chip width and height in pixels.

3.5 References

- [1] a) L. Zayat, C. Calero, P. Alborés, L. Baraldo, R. Etchenique, *J. Am. Chem. Soc.* **2003**, *125*, 882-883; b) P. J. Bednarski, F. S. Mackay, P. J. Sadler, *Anticancer Agents Med Chem* **2007**, *7*, 75-93; c) N. J. Farrer, L. Salassa, P. J. Sadler, *Dalton Trans.* **2009**, 10690-10701; d) U. Schatzschneider, *Eur. J. Inorg. Chem.* **2010**, *2010*, 1451-1467; e) S. L. H. Higgins, K. J. Brewer, *Angew. Chem., Int. Ed.* **2012**, *51*, 11420-11422; f) B. S. Howerton, D. K. Heidary, E. C. Glazer, *J. Am. Chem. Soc.* **2012**, *134*, 8324-8327; g) M. A. Sgambellone, A. David, R. N. Garner, K. R. Dunbar, C. Turro, *J. Am. Chem. Soc.* **2013**, *135*, 11274-11282.
- [2] a) M. Ferrari, *Nat. Rev. Cancer* **2005**, *5*, 161-171; b) Y. Matsumura, H. Maeda, *Cancer Res.* **1986**, *46*, 6387-6392.
- [3] a) T. N. Singh-Rachford, F. N. Castellano, *Coord. Chem. Rev.* **2010**, *254*, 2560-2573; b) J. Zhao, S. Ji, H. Guo, *RSC Adv.* **2011**, *1*, 937-950; c) Y. C. Simon, C. Weder, *J. Mater. Chem.* **2012**, *22*, 20817-20830; d) Y. Y. Cheng, B. Fückel, T. Khoury, R. I. G. C. R. Clady, N. J. Ekins-Daukes, M. J. Crossley, T. W. Schmidt, *J. Phys. Chem. A* **2011**, *115*, 1047-1053.
- [4] Y. Murakami, H. Kikuchi, A. Kawai, *J. Phys. Chem. B* **2013**, *117*, 2487-2494.
- [5] a) C. Wohnhaas, K. Friedemann, D. Busko, K. Landfester, S. Balushev, D. Crespy, A. Turshatov, *ACS Macro Lett.* **2013**, *2*, 446-450; b) R. R. Islangulov, J. Lott, C. Weder, F. N. Castellano, *J. Am. Chem. Soc.* **2007**, *129*, 12652-12653; c) P. B. Merkel, J. P. Dinnocenzo, *J. Lumin.* **2009**, *129*, 303-306; d) A. Monguzzi, R. Tubino, F. Meinardi, *J. Phys. Chem. A* **2009**, *113*, 1171-1174; e) T. N. Singh-Rachford, J. Lott, C. Weder, F. N. Castellano, *J. Am. Chem. Soc.* **2009**, *131*, 12007-12014.
- [6] a) A. Turshatov, D. Busko, S. Balushev, T. Miteva, K. Landfester, *New J. Phys.* **2011**, *13*, 083035; b) J.-H. Kang, E. Reichmanis, *Angew. Chem., Int. Ed.* **2012**, *51*, 11841-11844; c) J.-H. Kim, J.-H. Kim, *J. Am. Chem. Soc.* **2012**, *134*, 17478-17481; d) Q. Liu, B. Yin, T. Yang, Y. Yang, Z. Shen, P. Yao, F. Li, *J. Am. Chem. Soc.* **2013**, *135*, 5029-5037; e) K. Tanaka, H. Okada, W. Ohashi, J.-H. Jeon, K. Inafuku, Y. Chujo, *Bioorg. Med. Chem.* **2013**, *21*, 2678-2681; f) C. Wohnhaas, V. Mailänder, M. Dröge, M. A. Filatov, D. Busko, Y. Avlasevich, S. Balushev, T. Miteva, K. Landfester, A. Turshatov, *Macromol. Biosci.* **2013**, *13*, 1422-1430; g) Y. C. Simon, S. Bai, M. K. Sing, H. Dietsch, M. Achermann, C. Weder, *Macromol. Rapid Commun.* **2012**, *33*, 498-502.
- [7] J.-C. Boyer, F. C. J. M. van Veggel, *Nanoscale* **2010**, *2*, 1417-1419.

Chapter 3

- [8] a) R. N. A. H. Lewis, N. Mak, R. N. McElhaney, *Biochemistry* **1987**, *26*, 6118-6126; b) C.-H. Chang, H. Takeuchi, T. Ito, K. Machida, S.-i. Ohnishi, *J. Biochem.* **1981**, *90*, 997-1004; c) D. Marsh, *Handbook of Lipid Bilayers*, 2nd ed., Taylor & Francis Group, LLC, Boca Raton, FL, USA, **2013**.
- [9] a) S. Bonnet, B. Limburg, J. D. Meeldijk, R. J. M. Klein Gebbink, J. A. Killian, *J. Am. Chem. Soc.* **2010**, *133*, 252-261; b) R. E. Goldbach, I. Rodriguez-Garcia, J. H. van Lenthe, M. A. Siegler, S. Bonnet, *Chem. Eur. J.* **2011**, *17*, 9924-9929; c) A. Bahreman, B. Limburg, M. A. Siegler, R. Koning, A. J. Koster, S. Bonnet, *Chem. Eur. J.* **2012**, *18*, 10271-10280.
- [10] D. Needham, T. J. McIntosh, D. D. Lasic, *Biochim. Biophys. Acta, Biomembr.* **1992**, *1108*, 40-48.
- [11] K. J. Takeuchi, M. S. Thompson, D. W. Pipes, T. J. Meyer, *Inorg. Chem.* **1984**, *23*, 1845-1851.